Supporting Information

Berman et al. 10.1073/pnas.0902408106

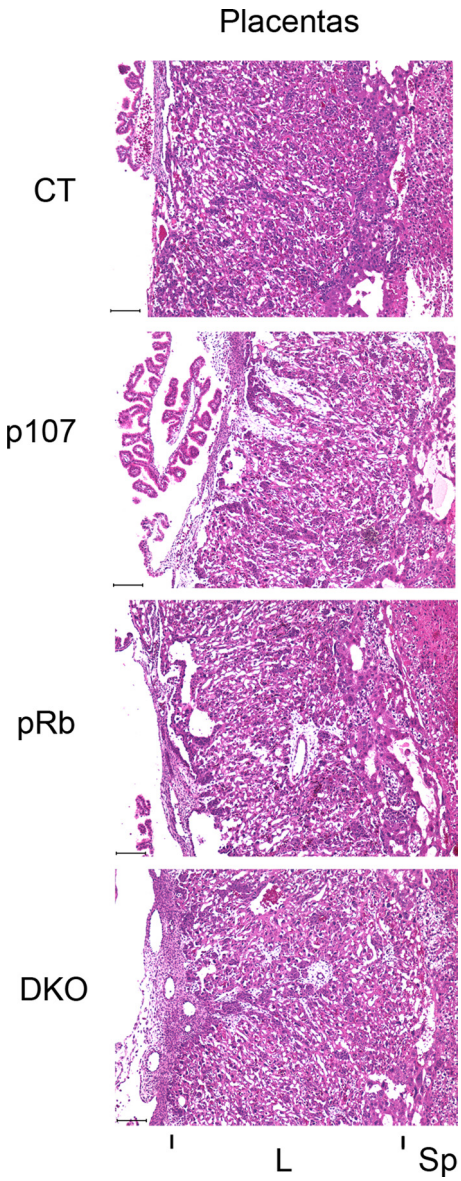

Fig. S1. Mutant embryos exhibit normal architecture within the labyrinth layer of the placenta. Sagittal sections through placentas of e13.5 embryos were examined. The double-mutant placentas were similar to control placentas and placentas of the other genotypes. In each panel, the maternal decidua is shown on the right and the chorion is shown on the left. (Scale bar: 100 μm.) L, labyrinth layer; SP, spongiotrophoblast layer.

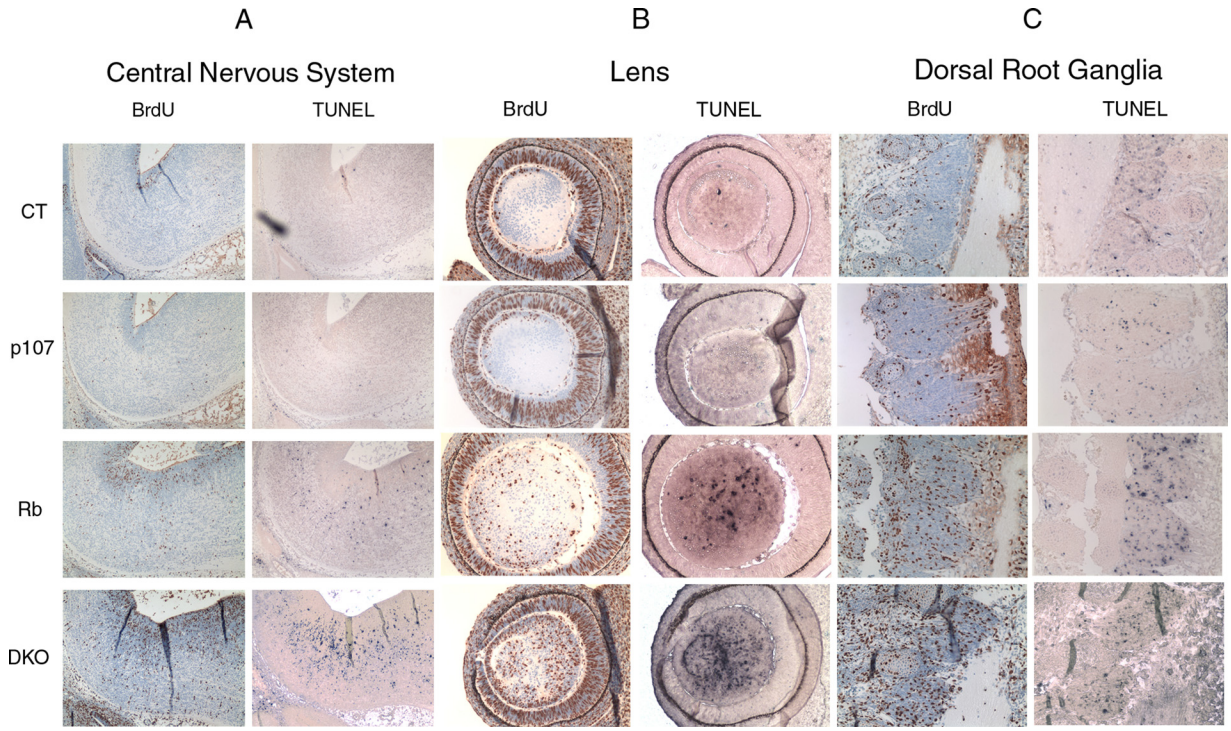

Fig. S2. Mutation of *p107* exacerbates the proliferative defects and apoptotis observed in the CNS and lens, but not in the PNS, of $Rb^{c-/c-}$ embryos. (*A* and *B*) Sagittal sections through the CNS (*A*) and lens (*B*) of e13.5 embryos were assessed by immunohistochemistry for BrdU incorporation, an indicator or proliferation, or by TUNEL for apoptosis. The $Rb^{c-/c-}$ CNS displayed an increase in proliferation and apoptosis, and mutation of *p107* exacerbates both phenotypes. (*C*) Sagittal sections through the dorsal root ganglia of e13.5 embryos were assessed for BrdU incorporation or apoptosis. $Rb^{c-/c-}$ ganglia displayed an increase in proliferation and apoptosis. The mutation of *p107* did not significantly affect these phenotypes. (Magnification: X20.) Quantification is shown in Fig. 1.

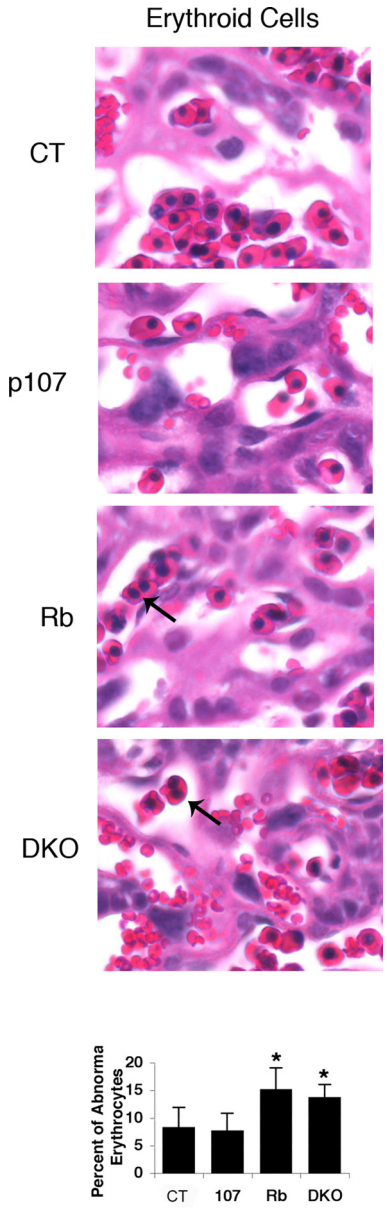

Fig. S3. $Rb^{c-/c-}$ and double-mutant embryos exhibit a similar percentage of abnormal erythroid cells. Sagittal sections through the placenta of e13.5 embryos were analyzed for the presence of abnormal fetal erythroid cells. (Magnification: X20.) Arrows indicate erythroid cells with multiple nuclei. Average percentage of abnormal nuclei is shown ($n \geq 4$ for each genotype). Error bars represent 1 SD. The asterisks denote statistical significance ($P < .05$) compared with control and $p107^{-/-}$ (*).

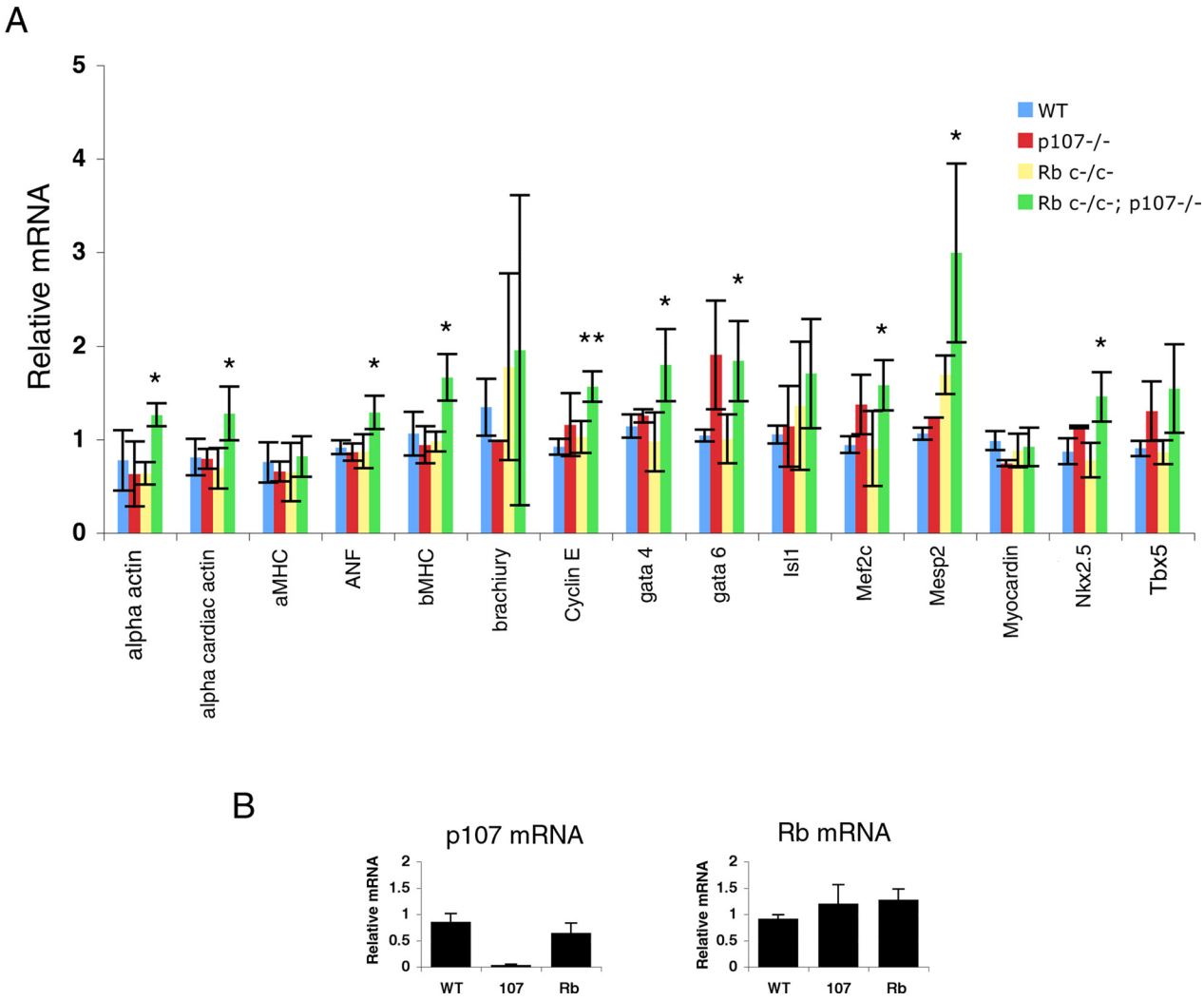

Fig. S4. (*A*) Mutant embryonic hearts (e13.5) exhibit no decrease in the expression of several cardiac markers on qRT-PCR. (*B*) No compensation at the transcriptional level by *Rb* or *p107* is seen in single-mutant embryos. qRT-PCR analysis shows that the *Rb* and *p107* mRNA levels are not significantly affected by mutation of *p107* or *Rb*, as assessed using the Student *t*-test ($P > .05$). Note that the mutation of *Rb* does not significantly reduce *Rb* mRNA levels. For both panels, RNA was isolated from the hearts of e13.5 embryos (control, $n = 3$; *Rb* mutant, $n = 2$; *107* mutant, $n = 2$; DKO, $n = 4$), reverse-transcribed, and subjected to qRT-PCR analysis. Ubiquitin was used as an internal control to normalize for mRNA levels within each sample. Error bars represent 1 SD. Statistical significance was determined using the Student *t*-test; * denotes $P < .05$, and ** denotes $P < .005$ when comparing DKO with control samples.

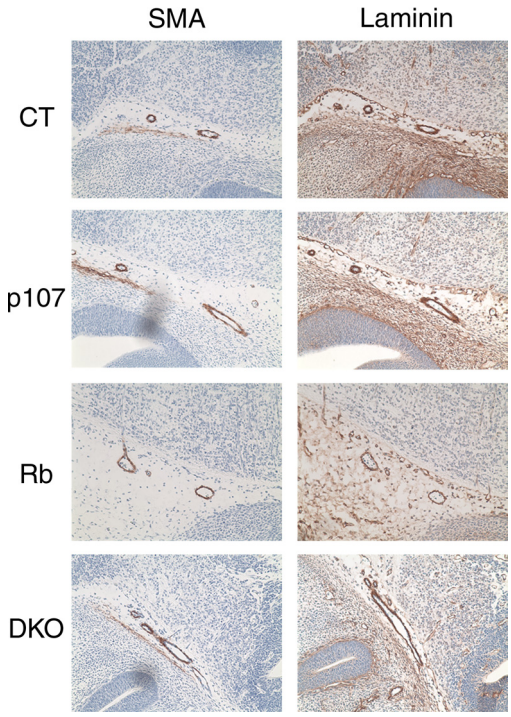

Fig. S5. DKO blood vessels exhibit normal marker expression. Sagittal sections of blood vessels of the head in e13.5 embryos were assessed by immunohistochemistry for smooth muscle actin and laminin expression. All embryos displayed normal expression of these blood vessel markers. (Magnification: X20.)

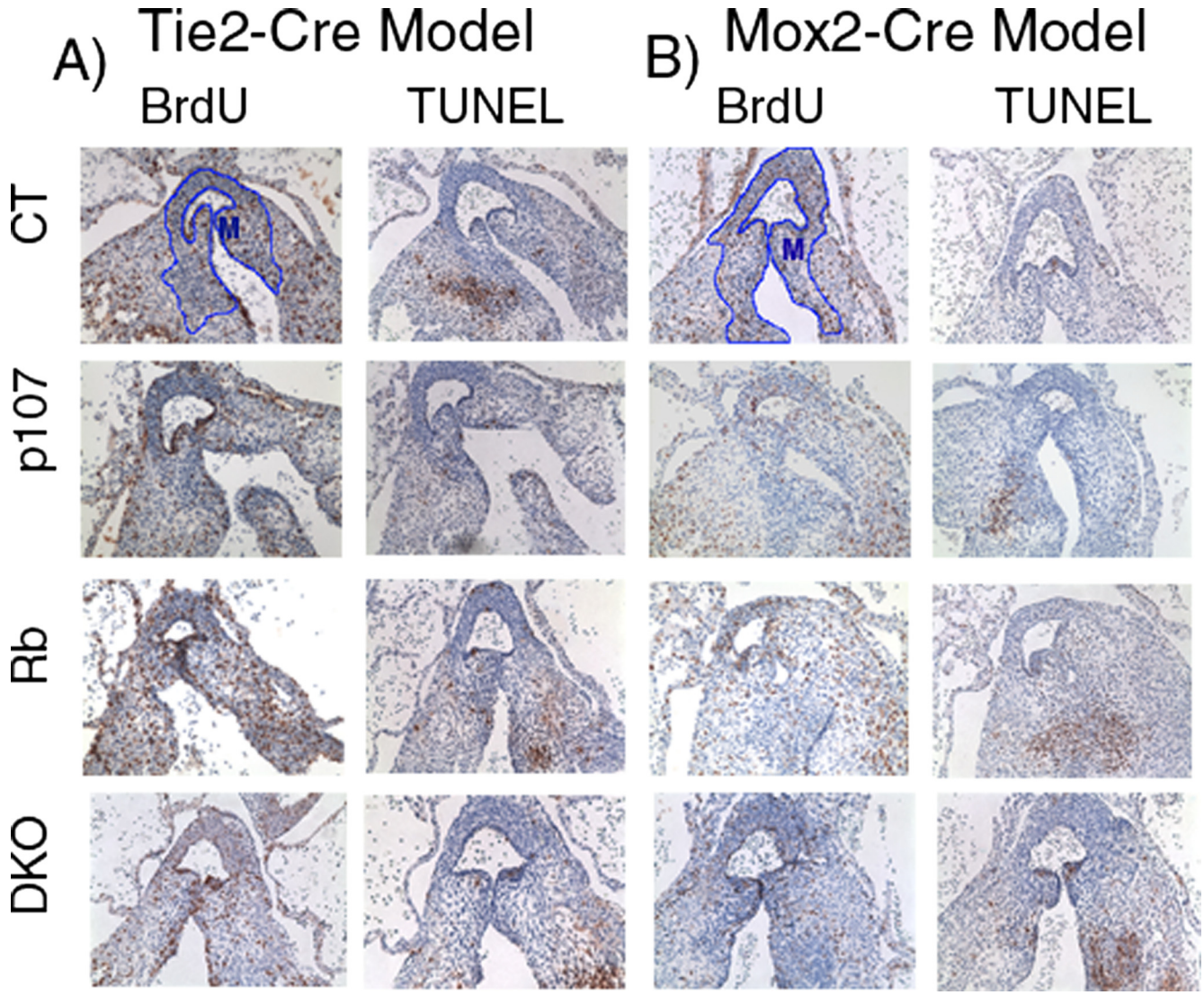

Fig. S6. Increased proliferation is seen in double-mutant heart endothelial cells. Transverse sections of e13.5 aortic valves were assessed by immunohistochemistry for incorporated BrdU or by TUNEL staining for apoptosis. (*A*) *Tie2-Cre* embryo heart sections of the 4 genotypes. (*B*) *Mox2-Cre* embryo heart sections of the 4 genotypes. (Magnification: X20.) Endothelial cells, mesenchymal cells, and cardiomyocytes were examined separately, and the percentage of cells exhibiting BrdU or TUNEL staining was quantified. The area demarcated in blue is the mesenchyme (M). Quantification is shown in Fig. 5.

Table S1. Primers used for quantitative RT-PCR analyses

	Forward 5′-3′	Reverse 5′-3′
Alpha actin	CACTGAAGCCCCGCTGAACG	TCGCCAGAATCCAGAACAATG
Alpha cardiac actin	AAGGCCAACCGTGAGAAGATGA	ATGGCAGGCACATTGAAGGTCT
AMHC	TTTGAGTGACAGAATGACGGACGC	TTGTCATCAGGCACGAAGCACT
ANF	AGTGGGCAGAGACAGCAAACAT	ACACCGCACTGTACACAGGATT
BMHC	ATTGGTGCCAAGGGCCTGAAT	TGCTTCCACCTAAAGGGCTGTT
Brachyury	GACTTCGTGACGGCTGACAA	CGAGTCTGGGTGGATGTAG
Cyclin E	TGTTTTTGCAAGACCCAGATGA	GGCTGACTGCTATCCTCGCT
Gata 4	AACGGAAGCCCAAGAACCTGAA	TGCTAGTGGCATTGCTGGAGTT
Gata 6	CCGCGAGTGCGTGAACT	CGCTTCTGTGGCTTGATGAG
Isl1	CATCGAGTGTTTCCGCTGTGTAG	GTGGTCTTCTCCGGCTGCTTGTGG
Mef2c	AGATACCCACAACACACCACGCGCC	ATCCTTCAGAGAGTCGCATGC
Mesp2	GTGCCTTTATCTGCCTCTTCTG	AGCGGGGGTGTCTTGTCTC
Myocardin	CATTGTTTCCCAAGGAGATTC	GCGATGTTACCCTCCTCAAAA
Nkx2.5	CATTTACCCGGGAGCCTACG	GCTTTCCGTCGCCGCCGTGCGCGTG
Tbx5	CCAGCTCGGCGAAGGGATGTTT	CCGACGCCGTGTACCGAGTGAT